Rational Design and Evaluation of New Lead Compound Structures for Selective βARK1 Inhibitors

Minoru Iino,[†] Taketoshi Furugori,[‡] Tomohiro Mori,[‡] Sachiko Moriyama,[‡] Akiko Fukuzawa,[‡] and Toshiro Shibano*,[‡]

Discovery Research Laboratories and New Product Research Laboratories II, Tokyo R&D Center, Daiichi Pharmaceutical Co., Ltd., 16-13 Kita-Kasai 1-Chome, Edogawa-ku, Tokyo 134-8630, Japan

Received March 2, 2001

β-Adrenergic receptor kinase 1 (βARK1) and cyclic adenosine 5′-monophosphate-dependent protein kinase A (PKA) have structurally similar adenine-binding pockets but have different physiologic functions. To obtain specific βARK1 inhibitors, a two step rational drug design process was used. First, a search was conducted on three-dimensional models of commercially available compounds to find compounds that fit the adenine-binding pocket of βARK1. Second, a comparative docking study that focused on the differences between the adenine-binding pockets of the two enzymes was used to evaluate the binding specificity of each compound that inhibited βARK1 activity. The results of these analyses yielded three βARK1-selective inhibitor leads from 11 candidates, a hit rate for selectivity of 27%. Although the IC_{50} values of these compounds for βARK1 ranged from only 1.3×10^{-4} M to 5.6×10^{-4} M, the compounds did not inhibit PKA at concentrations up to 1.0×10^{-3} M. Thus, the present study shows the usefulness of a rational drug design strategy in finding specific kinase inhibitors for proteins with similar drug target binding sites.

Introduction

A rational drug design process employs many techniques. These techniques, which include three-dimensional (3D) database searches and pharmacophore searches, have been successfully applied to select ligand candidates from chemical compound databases.[1−11] The present study uses a program named ARCHER, which was designed based on such algorithms,[12−15] to search for selective inhibitor leads of β-adrenergic receptor kinase 1 (βARK1). In addition to these techniques, Perola et al. objectively demonstrated the value or validity of their computational screening using a chemical database with a negative control study.[1] The present study also follows the negative control screening methodology of Perola et al. in order to assess the validity of the screening and design methods for finding selective inhibitor leads of βARK1.

βARK1 (EC 2.7.7.126) is a member of the G protein-coupled receptor kinase family.[16] Proteins that belong to this family affect a wide range of physiologic functions and participate in the pathogenesis of many chronic systemic disorders.[17] Indeed, by phosphorylating serine and threonine residues in the intracellular carboxyl terminal of β_2-adrenergic receptors bound to receptor agonists, βARK1 desensitizes β2-adrenergic receptors,[18] which is thought to contribute to the development of diseases such as congestive heart failure.[19−21] Thus, βARK1 inhibitors might prove to be powerful new drugs. However, any such compounds might inhibit other kinases, since many of these kinases are thought to have a structural similarity to βARK1. Therefore, the search for specific βARK1 inhibitors would benefit greatly from a rational, rather than random, screening and design process.

To conduct a computational drug screen properly, information on the tertiary structure and ligand recognition mechanism of the target molecule, in this case βARK1, is essential. Because this information is unknown, a previously proposed 3D model of the βARK1 catalytic domain was used.[22] This structure is based on a crystalline structure of cyclic adenosine 5′-monophosphate (AMP)-dependent protein kinase A (PKA; EC 2.7.1.37)−PKI5-24 complex, registered in the Protein Data Bank as 2CPK.[23] PKA is also a serine−threonine kinase. βARK1 and PKA share a 34.4% amino acid sequence identity in the catalytic domain. Additionally, PKA causes the desensitization of β_2-adrenergic receptors, as βARK1 does.[24] Furthermore, the amino acid residues at the adenosine 5′-triphosphate (ATP) binding site are highly conserved between βARK1 and PKA.[22] Consequently, the structure of PKA was used as a guide to construct a computer-generated 3D model of βARK1.

PKA specifically recognizes the $p-11$, $p-6$, $p-3$, $p-2$, and $p+1$ positions of the peptide inhibitor.[25] These positions are named in reference to Ala21, the phosphorylation site of peptide substrates designated p. Results from a previous study suggest that the PKA amino acid residues involved in the specific recognition of PKI5-24 at $s-11$, $s-6$, $s-2$, and $s+1$ sites are not conserved in βARK1 if the sites of PKA interacting with $p-n$ of PKI5-24 are designated as $s-n$.[22] Consequently, the specific ligand recognition sites of βARK1 were proposed to be $s-11$, $s-6$, $s-2$, and $s+1$.

In the present study, the strategy used to select potent and selective kinase inhibitors was to design compounds that interact with both the ligand recognition site and the adenine-binding pocket, a target site with high

* To whom correspondence should be addressed. Tel.: 3-3680-0151. Fax: 3-5696-8718. E-mail: shiba184@daiichipharm.co.jp.
[†] Discovery Research Laboratories.
[‡] New Product Research Laboratories.

10.1021/jm010093a CCC: $22.00
Published on Web 04/23/2002

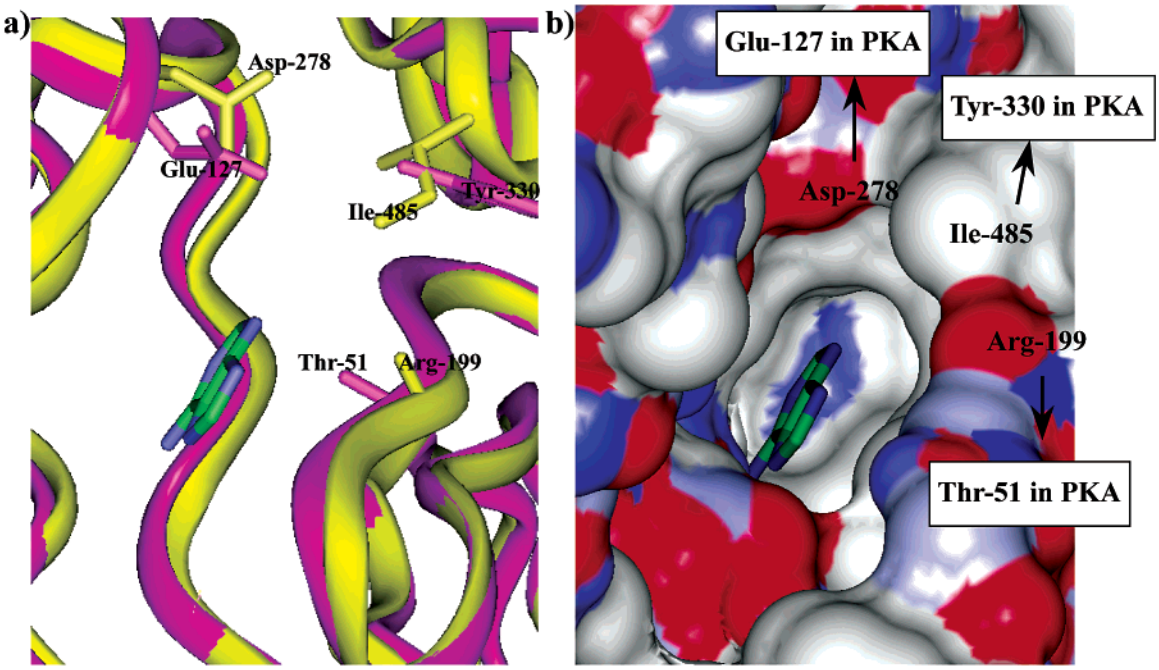

Figure 1. Ligand binding site with an adenine placed in reference to the PKA/PKI5-24/MgATP crystal structure.[58] (a) Comparison between βARK1 model structure and PKA crystal structure. Yellow, βARK1; pink, PKA. (b) Connolly surface drawings of βARK1 model structure.

Table 1. Distance from the Adenine Binding Site to Each Ligand Recognition Site in the βARK1 Model

ligand recognition site	representative atom	distance from Asp-272[a] (Å)
s−11	Ser-389 O_γ	27.3
s−6	Gly-355 C_α	25.6
s−3	Asp-278 C_γ	11.2
s−2	Lys-319 N_ζ	17.3
s+1	His-354 $N_{\epsilon 2}$	27.6

[a] Distances relative to the oxygen atom present in the Asp-272 main chain.

affinity for adenine in other kinases.[26,27] To use this strategy with a molecule as small as the candidate drug, the two sites cannot be too far apart from each other. However, the specific ligand recognition sites in βARK1, *s*−11, *s*−6, *s*−2, and *s*+1 are not suitable for designing selective inhibitor leads since, as listed in Table 1, they are located too far from the adenine-binding pocket of the ATP binding site. Therefore, another candidate site was needed.

In contrast with the *s*−11, *s*−6, *s*−2, and *s*+1 sites, the *s*−3 site is located next to the adenine-binding pocket in the previously proposed βARK1 model.[22] In this model, the *s*−3 site of βARK1 is surrounded by the main chain carbonyl group of Arg-199 and side chains of Asp-278 and Ile-485 (Figure 1).[28] The corresponding site in PKA is surrounded by the main chain carbonyl group of Thr-51 and side chains of Glu-127 and Tyr-330. The steric capacity and shape of βARK1 and PKA differ at this site in the following ways. First, Asp-278 in βARK1 and Glu-127 in PKA differ from each other in their side chain lengths. Second, there is a steric difference in van der Waals volume caused by the difference in side chains between Ile-485 in βARK1 and the corresponding Tyr-330 in PKA. Third, Thr-51 of PKA is slightly closer to Glu-127 than Arg-199 of βARK1 is to Asp-278. Consequently, a small molecule that can recognize these steric differences between βARK1 and PKA holds the potential to be a specific βARK1 inhibitor.

However, because the virtual screening method used in the present study does not directly compare the two enzymes, lead compound candidates selected by the virtual screening alone would not necessarily be specific to βARK1. To estimate their specificity to βARK1, comparative docking studies were used to find lead compound candidates with greater specificity for βARK1. This comparative docking study used superimposition of PKA structure on the putative βARK1−candidate complexes and qualitative estimation of repulsion between PKA and these candidates.

These facts and methods were used to form a rational drug design strategy to find specific βARK1 inhibitors and to confirm their activities. This process consisted of four steps: (i) potent βARK1 inhibitor lead compounds were found by pharmacophore-based virtual screening of a chemical structure database, (ii) the βARK1 inhibitory activity of these compounds was tested by an in vitro assay, (iii) the specificity of the candidate βARK1 inhibitors was tested by further docking studies with both βARK1 and PKA structures, and (iv) the PKA inhibitory activity of these compounds was tested by an in vitro assay.

Results

Pharmacophore Generation. In the process of pharmacophore probe generation, a hydrogen bond donor (HBD), a hydrogen bond acceptor (HBA), and an aromatic ring centroid (ARC) were defined after referring to the interaction between other kinases and their ligands. The final, simplified βARK1 pharmacophore model is shown in Figure 2. These pharmacophore probes were first used alone in the pharmacophore screening step and next used in combination with the

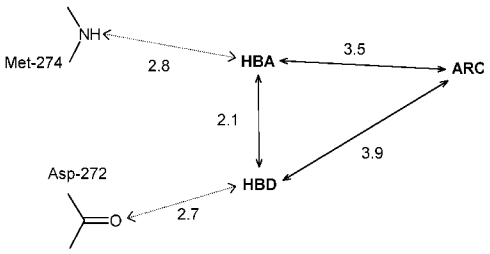

Figure 2. Schematic diagram outlining the ideal properties of a βARK1 pharmacophore. Numbers represent distances in Ångstroms.

Table 2. χ Angle (Reflecting Torsion around $C_\alpha-C_\beta$ Bond) of Four Amino Acid Residues in the Two Conformers of βARK1 and Their Corresponding Residues in the PKA Crystal Structure[a]

	Ile-197	Leu-271	Ser-334	Phe-483
βARK1 conformer 1	−70.2 (gauche+)	40.1 (gauche−)	−164.2 (trans)	−69.5 (gauche+)
βARK1 conformer 2	227.1 (trans)	−58.2 (gauche+)	−68.2 (gauche+)	−61.3 (gauche+)
	Leu-49	Met-120	Thr-183	Phe-327
PKA crystal structure	−58.4 (gauche+)	57.4 (gauche−)	−181.0 (trans)	−74.7 (gauche+)

[a] Unit: angular degree.

explicit βARK1 model structure to define the initial position for the automated docking analysis.

Modeling of βARK1 Conformers. In the βARK1 model building process, two models were adopted to reflect the flexibility of certain amino acid side chains. Their conformations differ from each other at the following amino acid residues: Ile-197, Leu-271, Ser-334, and Phe-483. The two models were defined as conformer 1 and conformer 2. The χ angle values (reflecting torsion around the $C_\alpha-C_\beta$ bond) for each residue of both conformers are summarized in Table 2. Conformer 1 was built during a previous study. This model was based on the crystalline structure of the PKA−PKI5-24 complex registered in the Protein Data Bank as 2CPK and was generated by the homology modeling method in the Protein Design module of the Quanta program.[29] To make conformer 2, the χ values of conformer 1 were modified manually to fit with more commonly reported χ angles.[30−32] This model was defined as conformer 2.

Database Search. The number of candidates that survived each step of the search is presented in Table 3. First, the Converter program[33] was used to generate 3D structures for 265 537 compounds of the original 267 733 compounds contained in the ACD 99.1 database.[34] Because the geometry check function of Converter resulted in a failure during the conversion calculation, the structures of 2196 of these compounds could not be generated. Converter also added 53 662 stereoisomers to the new database, making a total of 319 199 entries. Among these compounds, 263 334 had a molecular weight between 200 and 650, the target range. The next step was pharmacophore-based analysis of the database entries by ARCHER. The analysis yielded 134 652 compounds with functional groups that were compatible with the model pharmacophore. Of these 134 652 compounds, 112 314 compounds passed the distance matrix filter analysis. Following these analyses, automated flexible docking of the candidates

Table 3. Overview of the Search Process

search step	candidates remaining		
(1) original ACD	267 733		
(2) successful 3D structure calculation	265 537		
(3) addition of stereoisomers	319 199		
(4) molecular weight filtering (200−650)	263 334		
(5) carrying the pharmacophore's functional group	134 652		
(6) distance matrix fitness	112 314		
(7) successful docking to the βARK1 model	4387[a]		11 088[b]
(8) top scoring 2000 compounds	2000[a]		2000[b]
(9) unwanted functional group		3680	
(10) visual inspection: hydrogen bond formation, stable conformation, and hydrophobic interaction	361	662	614
(11) uniting multiple entries with the same ID		950	
(12) uniting entries with the similar chemical structure		280	
(13) final selection		11	

[a] Docking with the βARK1 conformer 1 model. [b] Docking with the βARK1 conformer 2 model.

to the βARK1 model was conducted by ARCHER. In this step, two conformers of βARK1 were used, and the calculations were named run 1 and run 2, after their respective conformers. The number of successfully docked compounds from run 1 was 4387 and from run 2 was 11 088. These docking models were evaluated by van der Waals and electrostatic energy terms calculated from the CHARMM function.[35] The top-scoring 2000 entries from each ARCHER run were put into one group and used in further analysis. Some compounds were contained in the results of both run 1 and run 2. In addition, this new group of 4000 compounds contained stereoisomers. Therefore, these 4000 entries were not necessarily unique chemical compounds but rather the best candidate docking modes with particular conformations and stereo configurations.

In-Depth Analysis. After the ARCHER search, compounds with unwanted chemical groups were discarded, reducing the total number of candidates from 4000 to 3680. Hydrogen bond formation and hydrophobic interaction were estimated by interatomic distances, and the top-scoring 1000 candidates from each category were selected for further analysis. The conformational stability of each candidate was also estimated by force field energy difference between the complexed conformation and freely minimized conformation, and the top-scoring 1000 candidates from this category were selected for further analysis. Compounds in each of the three categories were visually inspected to eliminate candidates without ideal hydrogen bond geometry, hydrophobic molecular surfaces, or torsion angles; this resulted in 361 candidates with good hydrogen bond geometry, 614 candidates with adequate hydrophobic surface area, and 662 candidates with proper torsion angles, respectively. These candidates were pooled, and redundant entries with the same chemical structure were represented by a single entry, reducing the total to 950. Some of these entries shared the same chemical substructures. For example, there were 111 xanthine derivatives, 155 adenine derivatives, 20 guanidine derivatives, and 121 uracil derivatives. Therefore, compounds with the same substructures were represented

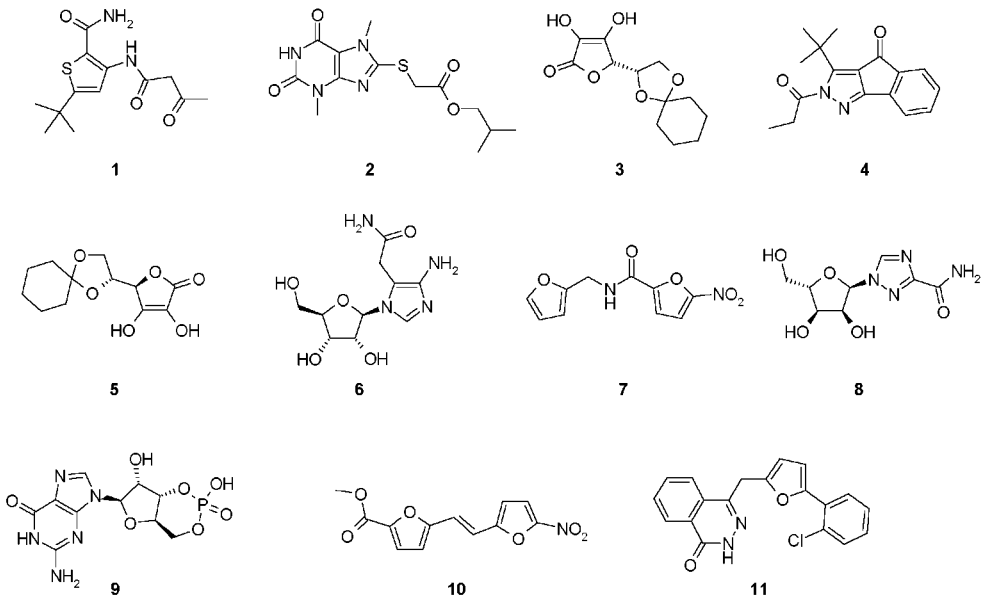

Figure 3. Chemical structures of the 11 candidate compounds selected from the database search for βARK1 inhibitors.

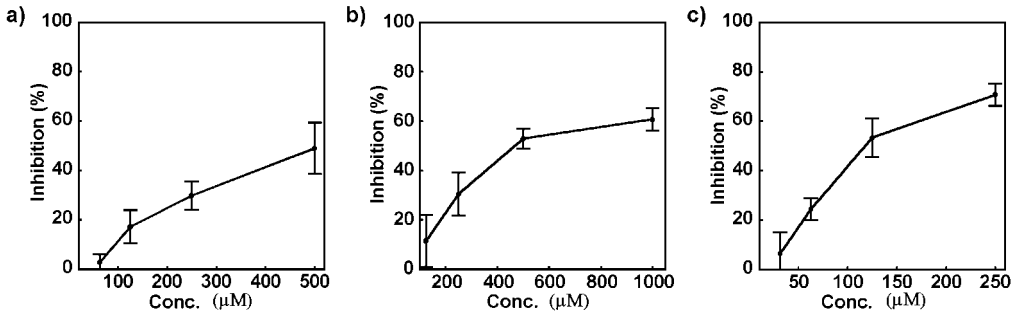

Figure 4. βARK1 inhibition by (a) compound **4**, (b) compound **6**, and (c) compound **10**. Data are expressed as mean ± SEM ($n = 6$).

Table 4. Inhibition of βARK1 Activity Caused by the 11 Selected Compounds and Their Calculated Interaction Energy When Complexed with βARK1

compd	calcd interaction energy (kcal/mol)	inhibition at 1 mM[a] (percentage of control value)	IC_{50} (μM)
1	−66.289	37.3	
2	−64.148	0.0	
3	−57.274	20.4	
4	−56.988	52.7	563
5	−55.882	0.0	
6	−55.211	60.7	557
7	−54.869	37.7	
8	−53.205	0.0	
9	−50.060	24.2	
10	−49.774	88.4	126
11	−37.878	67.3	

[a] Inhibition rate was regarded as zero if the calculated value was below zero.

by the top-scoring compounds. Compounds that were not commercially available were also eliminated. The resulting 280 compounds were inspected visually, and 11 compounds were selected to confirm their ability to inhibit βARK1 activity in an in vitro assay (Figure 3).

***β*ARK1 Inhibition Assay.** The in vitro βARK1 inhibitory activities of the 11 selected compounds are listed in Table 4. When tested at 1 mM during the first screening, four compounds inhibited βARK1 activity by more than 50%. Further assay of these compounds revealed that three compounds, 1-propionyl-8-oxo-9-tertiarybutyl-indenopirazole (compound **4**), 5-aminoimidazole-4-carboxamide 1-β-D-ribofuranoside (compound **6**), and methyl 5-[2-(5-nitro-2-furyl)vinyl]-2-furoate (compound **10**), have IC_{50} values in the range from 100 to 600 μM. None of these compounds have been previously reported to be βARK1 inhibitors. Additionally, the inhibition curves for these three compounds show concentration dependence (Figure 4), an indication of a real pharmacologic effect. In contrast, none of the randomly selected compounds (Figure 5) inhibited βARK1 activity by more than 50% at a concentration of 1 mM.

Selectivity Prediction. The graphical drawings for βARK1 and PKA complexed with different inhibitors show markedly different patterns (Figure 6). The adenine-binding pocket of βARK1 is large enough to accommodate the candidates without making contact with them. In contrast, in the drawing of the corresponding pocket of PKA, Thr-51 and Glu-127 sterically narrow the pocket or its entrance. The comparative docking study also focused on differences between Leu-271 in conformer 1 of βARK1 and Met-120 of PKA. Leu-271 of βARK1 can have two conformations: conformer 1 and conformer 2. In conformer 1, Leu-271 with a gauche(−) χ of 40.1° occupies almost the same space as Met-120 of PKA. In conformer 2, the χ of Leu-271 was modeled in gauche(+) form, −58.2°. Because of this change, the adenine-binding pocket of conformer 2 is larger than the adenine-binding pocket of conformer 1.

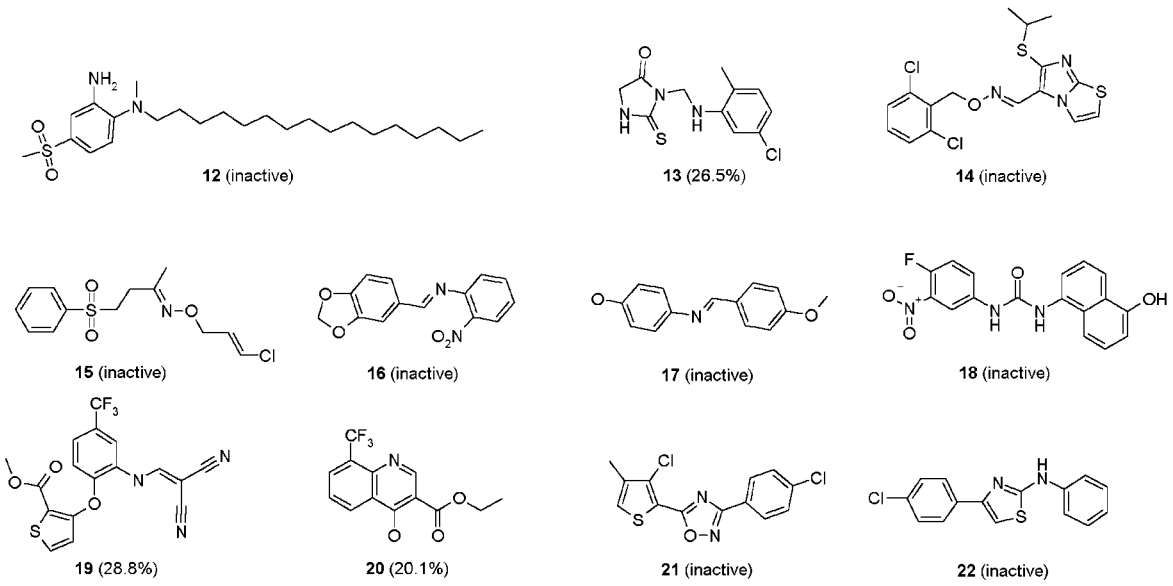

Figure 5. Chemical structures of the 11 compounds selected by a random number generator. The in vitro βARK1 inhibition activity at 1 mM is given in parentheses.

In model complexes with βARK1, none of the three molecules came into contact Asp-278, Ile-485, or Arg-199. In contrast to βARK1, PKA had less space in the binding site to accommodate the drug candidate molecules. The models predicted that compound **4** would come into contact with the side chain of Met-120 and the main chain of Thr-51. Compounds **6** and **10** would come into contact with the side chain of Glu-127. In addition, **10** might lose the CH$-\pi$ interaction because the Ile-485 of βARK1 is replaced by Tyr-330 in PKA. Thus, PKA is thought to have an unfavorable interaction with each of the three molecules because of steric differences between βARK1 and PKA, as shown in Figure 1.

PKA Inhibition Assay. To evaluate the selectivity of these compounds for βARK1 and not PKA, the in vitro inhibition of PKA activity caused by each of the three selected compounds was assayed (Table 5). These three compounds, **4**, **6**, and **10**, did not inhibit PKA activity even at concentrations of 1 mM. This contrasts with the IC_{50} value of the known PKA inhibitor PKI5-24, which is 0.003 μM.

Discussion

In the present study, the method applied yielded three inhibitors, **4**, **6**, and **10** (Figure 3), from 11 candidates while none of the randomly selected compounds inhibited βARK1 at a concentration of 1.0 mM. Computerized visual inspection predicted that none of these compounds would inhibit PKA, and assay results showed that they do not inhibit PKA at a concentration of 1.0 mM. This represents a hit rate for selectivity of 27%. While the best IC_{50} value for this group of compounds is 1.3×10^{-4} M, these compounds are the first low molecular weight inhibitors that can specifically distinguish βARK1 from PKA. Thus, the results show, at least for the present target protein, that using a search on a database containing 3D structures and a comparative docking study can detect specific protein inhibitors.

At the same time, however, the results suggested room for improvement. For example, the estimated interaction energy ranking was thought not to parallel the biological activity accurately. There are several possible reasons for this discrepancy. First, the stability estimation of the protein$-$ligand complex depended on the force field energy function. Generally, such force field energy functions only calculate enthalpy, while entropic terms such as flexibility and hydrophobic interactions might consume a significant portion of the free energy.[36,37] Better results might be obtained by adopting empirical free energy scoring functions.[38−40] In the present study, however, these functions were not used because the functions cannot be differentiated easily, resulting in larger calculation times. Second, the docking method used in this study did not cover all conformations; therefore, the best docking mode for each molecule might have been overlooked. More precise calculations might yield better results. However, such calculations were not used because the goal of this study was not a precise docking study for each molecule but rather a search to pick up inhibitor candidates by means of a realistic and feasible process of calculation. Third, during the database search, the protein structure that bound the target pharmacophore was assumed to be rigid. This assumption made it difficult to reflect the flexibility of amino acids on the surface of the protein in the final assessment.[41−43] Using multiple conformers of the target protein might increase the probability of selecting more compounds, and actually, two models were adopted in the present study. Actually, βARK1 conformer 1 identified only compound **6** while conformer 2 identified all of the three selective inhibitor leads. Therefore, the use of only conformer 1 would have overlooked compounds **4** and **10**. Thus, an increase in the number of models might lead to more accurate results. Fourth, Because PKA changes its conformation according to bound molecules,[44] βARK1 would also change it like PKA does. In the present study, the βARK1 structure was modeled based on the PKA$-$PKI binary complex crystal structure in which PKA adopts a "closed" conformation[45] and the empty ATP binding site is in its native form. Because the virtual screening

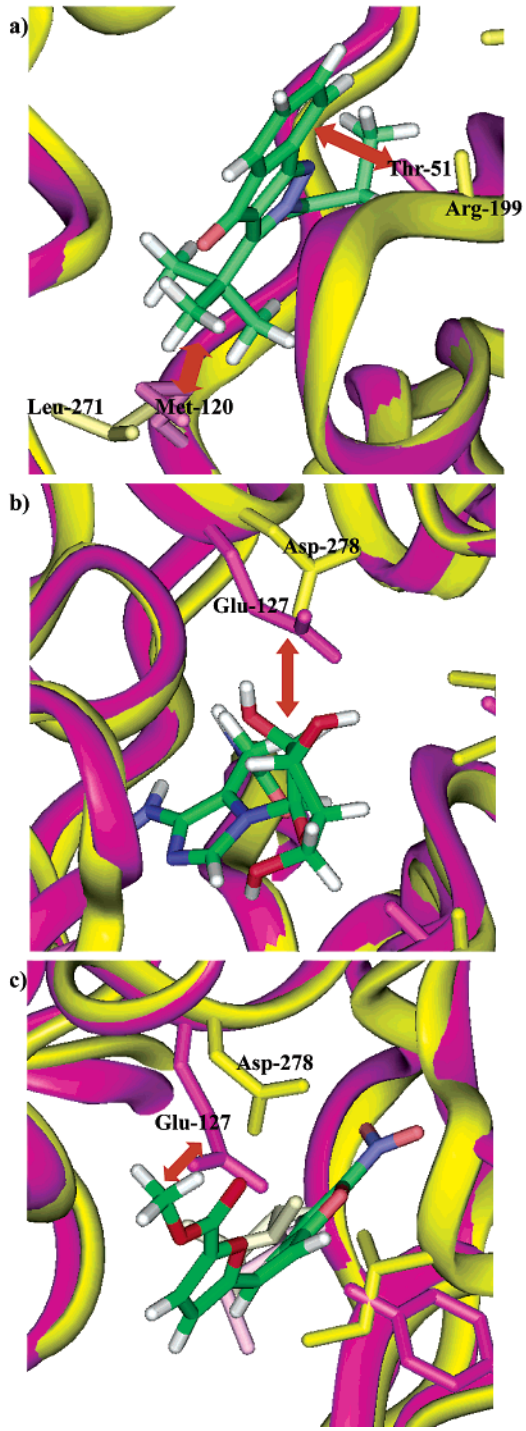

Figure 6. Structural comparison of βARK1 or PKA in complex with βARK1 inhibitors. Yellow, βARK1; pink, PKA. Putative intermolecular repulsion is shown by an orange arrow. (a) Compound **4**, (b) compound **6**, and (c) compound **10**.

using this model identified three selective inhibitor leads, it would reflect a βARK1 conformation. In addition, βARK1 models based on other PKA crystal structures would reproduce different conformations of βARK1, which would diversify the variety of inhibitors resulting from the virtual screening. Fifth, the 3D structure of the target protein was a calculated model because there are no data describing the 3D structure of βARK1. The accuracy of such models derived from homology modeling depends on how similar the modeled protein is to the reference protein. In the present study, the amino acid identity of the modeled region between βARK1 and PKA was 34.4%. With such a relatively low identity, the modeled structure might have inaccurate side chain orientations or main chain folding,[46] which would deleteriously affect the overall rational drug design process. Finally, it is also possible that other regions not modeled play a significant role in ligand binding.

Table 5. PKA Inhibitory Activity of Compounds **4**, **6**, and **10**

compd	inhibition (percentage of control value)
4	−2.2% at 1 mM
6	−6.5% at 1 mM
10	1.8% at 1 mM
PKI 5-24[a]	IC_{50} = 0.003 μM

[a] Positive control compound.

In the step following the 3D database search, the binding specificity of the inhibitor for βARK1 and PKA was examined visually based on the structures of the putative protein−compound complexes. There were marked steric differences between the ATP binding site of the βARK1 model structure and PKA crystalline structure. These differences were important to the present study since intermolecular contact could be predicted through a graphical representation technique such as molecular surface drawing. The comparison between βARK1 and PKA through superposition presupposes that all inhibitors of these proteins that act at this site have a common binding mechanism. This is a likely assumption since there are several examples in which the binding mechanism of a ligand is conserved between proteins with similar structures and functions.[47,48] However, the visual comparison process was qualitative and not quantitative. This process should be replaced with an objective method as soon as a scoring function with enough accuracy is developed.

The activity of the inhibitors obtained in the present study is not as potent as the activity usually observed for medicines. Their physical and chemical properties were also not favorable for clinical use because of moieties such as nitro groups or sugar substructures. Thus, the next step is to optimize the chemical structures of the compounds to achieve higher affinity for βARK1 and better bioavailability. Because the putative 3D structural information is already available for complexes between βARK1 and the inhibitors, the modification process to increase affinity and selectivity will likely be rapid. The process of molecular design to obtain favorable properties will probably involve remodeling of the tertiary butyl group of compound **4**, replacement of the sugar scaffold of compound **6**, and substitution of the nitro group of compound **10** by other chemical groups with the similar geometry and interaction properties. As these compounds are modified, the models of the complexes will provide the geometric information necessary to make appropriate changes.

Conclusions

In conclusion, specific βARK1 inhibitor candidates were obtained from a search of a database containing 3D drug candidate structures, followed by a comparative docking study. The inhibitor candidates resulting from this screening inhibited βARK1 without affecting PKA activity. Indeed, these are the first small size selective inhibitor leads of βARK1 ever reported. The results of

the present study demonstrate the effectiveness of a combined strategy of 3D database search and a consecutive comparative docking study for identifying selective inhibitor leads for βARK1 and indicate its general usefulness for other systems.

Experimental Section

Materials. PKA and a colorimetric PKA assay kit were purchased from Pierce (Rockford, IL). The PKA inhibitor PKI5-24 was purchased from Biomol Research Laboratories, Inc. (Plymouth Meeting, PA). The structures of the compounds assayed are shown in Figures 3 and 5. Compounds **1**, **7**, **13**, **19**, **21**, and **22** were purchased from Maybridge (Cornwall, U.K.); compounds **2**, **12**, **16**, and **18** were purchased from SALOR (Sigma Aldrich Library of Rare Chemicals; Aldrich Chemical Co. Inc.; Milwaukee, WI); compound **3** was purchased from Aldrich; compound **4** was purchased from Menai (N. Wales, U.K.); compound **5** was purchased from Fluka (Milwaukee, WI); compounds **6**, **8**, and **9** were purchased from Sigma (St. Louis, MO); compounds **10**, **11**, **14**, **15**, and **20** were purchased from Bionet (Cornwall, U.K.); and compound **17** was purchased from TCI (Tokyo, Japan).

Hardware and Software. Four personal computers (each having two Pentium II 450 MHz processors) running the Red Hat Linux 5.2 operating system were used to develop and run the ARCHER program. A Silicon Graphics Octane (R10000 195 MHz processor) computer running the IRIX 6.5.3 operating system was used to draw and manipulate molecular structures. An IBM RS/6000 running the AIX 4.1.4 operating system was used as the ISIS/Host 2.2.1h server, and a PC (Pentium 120 MHz processor) running Windows 95 was used as the ISIS/Base 2.2.1h client. The ISIS/Base[49] program was used as the database filtering software. The Quanta 97 program was used to calculate Connolly surfaces to visualize molecules and to draw molecular structures. The Insight II 98.0 program[50] was used to fill hydrogen and to run the CHARMM program, and the Converter program, which is a module of the Insight II software suite, was used to generate the 3D structures. The Cerius 2 program[51] was used to group molecules. To filter and search compounds in the chemical database, an in-house program named ARCHER (Automatic and Rational Complementary Hit-compound ExploreR) was developed.

Pharmacophore Generation. To streamline the initial docking calculation between βARK1 and candidate compounds, the complexity of the putative target site on βARK1 was simplified into a pharmacophore model consisting of elements such as HBDs, HBAs, and ARCs, based on the following observations. In the adenine-binding pocket of PKA, the amide oxygen of Glu-121 and the amide nitrogen of Val-123 form strong and specific hydrogen bonds with ATP.[24] Therefore, the corresponding atoms in βARK1, which were the amide oxygen of Asp-272 and the amide nitrogen of Met-274, were used to define pharmacophore points in βARK1 for hydrogen bonds similar to those observed in a PKA−ligand complex. For the amide oxygen of Asp-272, an HBD was placed 2.8 Å, a standard hydrogen bond length, from the oxygen in the sp2 plane with the lone electron pair pointing in the direction of the oxygen. For the amide nitrogen of Met-274, an HBA was placed 2.8 Å, a standard hydrogen bond length, from the nitrogen in the sp2 plane with the hydrogen bond pointing in the direction of the nitrogen. Then, to remove short contacts, the position of each HBD and HBA was optimized while the βARK1 position remained fixed through a CHARMM force field calculation. In the calculation, the HBD was assumed to have the characteristics of an sp3 nitrogen atom, and the HBA was assumed to have the characteristics of an sp3 oxygen atom. Additionally, in the adenine-binding pocket of PKA and other kinases, an aromatic ring system is recognized specifically.[52] Assuming the same recognition mechanism operates in βARK1, an ARC was placed by referring to aromatic ring center coordinates of other known kinase−ligand complex structures in the PDB such as 1BKX, 1STC, 1YDS, and 1YDT. Then, to remove unfavorable contacts between the compounds and the enzymes, the position of the ARC was optimized while the βARK1 position remained fixed through a CHARMM force field calculation. In the calculation, the ARC was assumed to have the characteristics of an sp3 carbon atom.

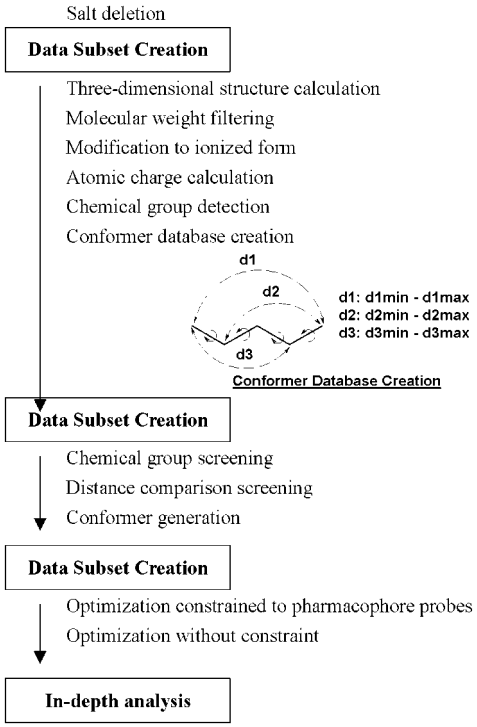

Figure 7. Outline of ARCHER procedure.

Database Search. The pharmacophore search and protein-docking analysis algorithms of the ARCHER program were derived from those of ISIS/Base[12] and other previously reported programs[13−15] with some modifications. Figure 7 shows the outline of the ARCHER calculations. The ARCHER procedure consists of three steps. The first step is initial candidate selection by filtering and structure modifications that include 3D structure generation; the second step is a pharmacophore-based conformationally flexible database search; and the third step is a docking study using the target proteins. Because of licensing restrictions, all files containing molecular information were saved only temporarily and were used only as a means of passing information between programs.

In the first step, a data subset was created by the following filtering process. The Available Chemical Directory (ACD) 99.1 was used as the database of commercially available compounds.[53] Unique molecules were isolated by taking only the largest molecule for any particular formula entry while other molecules in the same entry were regarded as salt molecules and were removed. After these redundant salts were removed, the Insight II/Converter software suite was used to fill in all possible hydrogen atoms and convert the formula into a 3D structure. For compounds with several racemic centers, at most four arbitrary stereoisomers were generated and each resulting structure was treated as a new database entry. Molecules for which a 3D structure could not be calculated by Converter were discarded. A molecular weight range from 200 to 650 was defined as the preferred range for drug molecules and was also used as a cardinal condition of a filtering process. Acidic functional groups such as carboxylic acid, sulfonic acid, and phosphoric acid were deprotonated, and basic groups such as amines, amidines, and guanidines were protonated. Gasteiger's atomic charges[54] were also calculated. Finally, possible conformations were generated systematically but temporarily by rotation of freely rotatable bonds. During conformation generation, all pairs of interatomic distances between HBD, HBA, and ARC were recorded. Then, a database of distance ranges for every possible combination of HBD, HBA, and ARC was created.

In the second step, a pharmacophore search was performed on this initial candidate group. The search consisted of the following procedures. First, the pharmacophore elements were used to select qualified compounds that possess the needed number and kind of functional groups for the current pharmacophore, using the key screening algorithm in the ISIS/Base program[12] and the formula screen algorithm in the ChemDBS-3D program.[13] At this stage, molecules with at least two of the pharmacophore elements were selected. Second, the upper and lower distance range database of resulting candidates was screened with the distance matrix of the model pharmacophore, revealing whether a candidate compound was comparable with the pharmacophore. This method was inspired from the minimum residual algorithm used in the FLOG program.[14] Third, conformers were generated systematically for each candidate and superimposed onto the pharmacophore model by rigid body rotation and translation. The goodness-of-fit of each conformer to the model pharmacophore was assessed by root mean square distance calculations between the pharmacophore elements and the corresponding points of the conformer.

In the third step of the filtering process, force field calculations were applied to minimize the energy of each conformer generated to fit the βARK1 pharmacophore model. ARCHER scored each compound using eq 1 and 2

$$E = \sum_{i,j>i} \frac{q_i q_j}{4\pi\epsilon_0 {r_{ij}}^2} + \sum_{i,j>i} \epsilon_{ij}^* \left[\left(\frac{r_{ij}^*}{r_{ij}} \right)^{12} - 2 \left(\frac{r_{ij}^*}{r_{ij}} \right)^{6} \right] \quad (1)$$

$$\epsilon_{ij}^* = (\epsilon_i^* \epsilon_j^*)^{1/2},\ r_{ij}^* = r_i^* + r_j^* \quad (2)$$

where q is the atomic charge, r is the interatomic distance, ϵ_0 is the dielectric constant, and ϵ is the van der Waals constant. An asterisk means a standard value of the force field. The force field parameters and functions were taken from the CHARMM program. The grid energy calculation method was used to calculate intermolecular interaction energy, and βARK1 was treated as a rigid protein. To reflect the flexibility of certain amino acid side chains, two conformational models of βARK1 were constructed. Search calculations using each model were named run 1 and run 2, respectively. Energy minimization of each candidate−βARK1 complex consisted of two phases. The first phase was energy minimization of the candidate compound constrained by the superimposed pharmacophore, and the second phase was nonconstrained minimization. Ligand translation was limited within the extents of the grid, similar to the function used in the AutoDock program.[15] After these minimization processes, the 2000 top-scoring candidates from run 1 and run 2 proceeded to further analysis. These 4000 candidates contained the entries with the same chemical structure but different chiral center configurations and different docking orientations.

In-Depth Analysis. Candidates resulting from the ARCHER search were analyzed further. First, candidates with unwanted functional groups such as acid halides, acid anhydrides, aldehydes, azides, isocyanates, thiocyanates, epoxides, and thiols were eliminated. Then, each candidate was evaluated with the following three measurements: (i) the distances of hydrogen bonds formed by the amide oxygen of Asp-272 or formed by the amide nitrogen of Met-274, (ii) the number of aliphatic and aromatic carbons within 4.0 Å from side chains of Ile-197, Val-205, Ala-218, Met-274, Leu-324, and Phe-483, and (iii) the force field energy difference between the complexed conformation and the minimized conformation calculated from the complexed conformation. The top-scoring 1000 candidates from each category were then inspected to eliminate candidates with unrealistic hydrogen bond geometry, discontinuous hydrophobic molecular surfaces, or unstable torsional configuration, respectively. The candidates in each category were united as a group. Then, entries selected from both run 1 and run 2, redundant stereoisomers, and entries that are not commercially available were eliminated. Compounds with similar chemical structures were also eliminated after clustering by the Cerius2 program and substructure search by the ISIS/Base program. The resulting candidates were visually inspected on the computer display to make the final selection.

Negative Control. As a negative control group, 11 compounds were selected randomly from the 263 334 entries, which was the entry list just before the pharmacophore search. A random selection script using the rand function written in Perl 5.005 was run on Red Hat Linux 6.2 to select the compounds.

***β*ARK1 Inhibition Assay.** The inhibition of βARK1 activity caused by each test compound was assayed using a previously reported method, with some modifications.[55] A reaction mixture containing 10 mM [γ-^{32}P]ATP (18.5 kBq), the intracellular carboxyl terminal domain of the human β2-adrenergic receptor (6.7 μM), and either one concentration (range: 2.0−6.0 μg/mL) of βARK1 or a blank solution (as a control) were incubated in reaction buffer (20 mM Tris-HCl, pH 7.5; 5 mM $MgCl_2$; 2 mM EDTA; 0.5 mM EGTA) at 30 °C for 60 min. After the phosphorylation reactions were stopped by immersing the test tubes in ice water, electrophoresis was used to separate the components of the reaction mixture, and an Imaging Plate (Fujifilm, Japan) was used to record the distribution pattern of radioactivity on the electrophoresis gel. A BAS 2000 bioimage analyzer (Fujifilm, Japan) was used to read the Imaging Plate. During the initial screening, the concentration of each compound was 1 mM and only one reaction was conducted per candidate compound. The secondary screening was conducted with six replicates of four different concentrations for each candidate compound. The percentage inhibition rate was calculated by eq 3

$$\text{inhibition} = \frac{R_{\text{control}} - R_{\text{sample}}}{R_{\text{control}} - R_{\text{background}}} \times 100 \quad (3)$$

where R_{sample}, R_{control}, and $R_{\text{background}}$ are the radioactivity in the assayed sample, positive control, and background samples, respectively. The percentage inhibition rate was recorded as zero if the calculated value was below zero.

Selectivity Prediction. After finding potential βARK1 inhibitors, their ability to inhibit PKA was estimated by superimposing the crystalline structure of PKA, registered in the Protein Data Bank as 2CPK, onto the βARK1−candidate complex model in the same coordinate system. Then, a structural comparison, which has been successfully applied to estimate ligand selectivity,[56,57] was applied to βARK1 and PKA. The major steric difference between Asp-278 of βARK1 and Glu-127 of PKA was visualized by means of a Connolly surface image (probe radius: 1.4 Å). Because force field energy depends on the number of atoms included in the system, absolute force field energies could not be compared between PKA and βARK1. Therefore, a comparative docking study and visual examination were used to perform qualitative analysis instead of using a quantitative assessment such as energy calculation. Using interatomic distance information and atomic charge information, candidates with short contact with the enzyme except for hydrogen-bonding atoms or with electrostatic pattern mismatches were judged to be unfavorable for PKA binding.

PKA Inhibition Assay. The inhibition of PKA activity caused by each test compound was assayed using a colorimetric PKA assay kit. PKI5-24 was used as the positive control inhibitor for PKA. The assay was performed according to the directions supplied with the kit. A test compound, PKA (final activity: 87 units/μL), and the dye-linked PKA substrate (kemptide, sequence: LRRASLG) were incubated in reaction buffer (2 mM ATP, 10 mM $MgCl_2$, 0.002% Triton X-100, 20 mM Tris(hydroxymethyl)amino methane, 100 mM cAMP, 5% DMSO, pH 7.4) for 30 min at 30 °C. After the reaction was terminated, the phosphorylated dye-linked substrate was selectively trapped by an affinity membrane, was isolated by means of the elution buffer supplied with the kit, and was quantified by OD measurement at 570 nm. Optical density was

measured by means of a Spectra Max 340 spectrophotometer (Molecular Devices Corp., CA).

Acknowledgment. We thank Mr. Steven E. Johnson for editing the manuscript.

Supporting Information Available: Coordinates for each candidate (compound 1−11) and adenine-binding pocket of βARK1 conformer 1 and conformer 2. This material is available free of charge via the Internet at http://pubs.acs.org.

References

(1) Perola, E.; Xu, K.; Kollmeyer, T. M.; Kaufmann, S. H.; Prendergast, F. G.; Pang, Y.-P. Successful Virtual Screening of a Chemical Database for Farnesyltransferase Inhibitor Leads. *J. Med. Chem.* **2000**, *43*, 401−408.

(2) Wang, S.; Sakamuri, S.; Enyedy, I. J.; Kozikowski, A. P.; Deshaux, O.; Bandyopadhyay, B. C.; Tella, S. R.; Zaman, W. A.; Johnson, K. M. Discovery of a Novel Dopamine Transporter Inhibitor, 4-Hydroxy-1-methyl-4-(4-methylphenyl)-3-piperidyl 4-Methylphenyl Ketone, as a Potential Cocaine Antagonist through 3D-Database Pharmacophore Searching. Molecular Modeling, Structure−activity Relationships, and Behavioral Pharmacological Studies. *J. Med. Chem.* **2000**, *43*, 351−360.

(3) Kuntz, I. D Structure-based strategies for drug design and discovery. *Science* **1992**, *257*, 1078−1082.

(4) Shoichest, B. K.; Stroud, R. M.; Santi, D. V.; Kuntz, I. D.; Perry, K. M. Structure-based discovery of inhibitors of thymidylate synthase. *Science* **1993**, *259*, 1445−1450.

(5) Rutenber, E.; Fauman, E. B.; Keenan, R. J.; Fong, S.; Furth, P. S.; Ortiz de Montellano, P. R.; Meng, E.; Kuntz, I. D.; DeCamp, D. L.; Salto, R. Structure of a non-peptide inhibitor complexed with HIV-1 protease. Developing a cycle of structure-based drug design. *J. Biol. Chem.* **1993**, *268*, 15343−15346.

(6) Zheng, Q.; Kyle, D. J. Computational screening of combinatorial libraries. *Bioorg. Med. Chem.* **1996**, *4*, 631−638.

(7) Gschwend, D. A.; Good, A. C.; Kuntz, I. D. Molecular docking towards drug discovery. *J. Mol. Recognit.* **1996**, *9*, 175−186.

(8) Finn, P. W. Computer-based screening of compound databases for the identification of novel leads. *Drug Discovery Today* **1996**, *1*, 363−370.

(9) Horvath, D. A virtual screening approach applied to the search for trypanothione reductase inhibitors. *J. Med. Chem.* **1997**, *40*, 2412−2413.

(10) Toyoda, T.; Brobey, R. K. B.; Sano, G.; Horii, T.; Tomioka, N.; Itai, A. Lead Discovery of Inhibitors of the Dihydrofolate Reductase Domain of Plasmodium Falciparum Dihydrofolate Reductase-Thymidylate Synthase. *Biochem. Biophys. Res. Commun.* **1997**, *235*, 515−519.

(11) Walters, W. P.; Stahl, M. T.; Murcko, M. A. Virtual screening—an overview. *Drug Discovery Today* **1998**, *3*, 160−178.

(12) Moock, T. E.; Henry, D. R.; Ozkabak, A. G.; Alamgir, M. Conformational Searching in ISIS/3D Databases. *J. Chem. Inf. Comput. Sci.* **1994**, *34*, 184−189.

(13) Murrall, N. W.; Davies, E. K. Conformational Freedom in 3-D Databases. 1. Techniques. *J. Chem. Inf. Comput. Sci.* **1990**, *30*, 312−316.

(14) Miller, M. D.; Kearsley, S. K.; Underwood, D. J.; Sheridan, R. P. FLOG: A system to select "quasi-flexible" ligands complementary to a receptor of known three-dimensional structure. *J. Comput.-Aided Mol. Des.* **1994**, *8*, 153−174.

(15) Morris, G. M.; Goodsell, D. S.; Huey, R.; Olson, A. J. Distributed automated docking of flexible ligands to proteins: Parallel applications of AutoDock 2.4. *J. Comput.-Aided Mol. Des.* **1996**, *10*, 293−304.

(16) Sibley, D. R.; Benovic, J. L.; Caron, M. G.; Lefkowitz, R. J. Regulation of Transmembrane Signaling by Receptor Phosphorylation. *Cell* **1987**, *48*, 913−922.

(17) Premont, R. T.; Inglese, J.; Lefkowitz, R. J. Protein kinases that phosphorylate activated G protein-coupled receptors. *FASEB J.* **1995**, *9*, 175−182.

(18) Lohse, M. J.; Lefkowitz, R. J.; Caron, M. G.; Benovic, J. L. Inhibition of β-adrenergic receptor kinase prevents rapid homologous desensitization of β2-adrenergic receptors. *Proc. Natl. Acad. Sci. U.S.A.* **1989**, *86*, 3011−3015.

(19) Ungerer, M.; Bohm, M.; Elce, J. S.; Erdmann, E.; Lohse, M. J. Altered Expression of β-Adrenergic Receptor Kinase and β1-Adrenergic Receptors in the Failing Human Heart. *Circulation* **1993**, *87*, 454−463.

(20) Ungerer, M.; Parruti, G.; Bohm, M.; Puzicha, M.; DeBlasi, A.; Erdmann, E.; Lohse, M. J. Expression of β-Arrestins and β-Adrenergic Receptor Kinases in the Failing Human Heart. *Circ. Res.* **1994**, *74*, 206−213.

(21) Koch, W. J.; Rockman, H. A.; Samama, P.; Hamilton, R. A.; Bond, R. A.; Milano, C. A.; Lefkowitz, R. J. Cardiac Function in Mice Overexpressing the β-Adrenergic Receptor Kinase or a βARK Inhibitor. *Science* **1995**, *268*, 1350−1353.

(22) Iino, M.; Shibano, T. SUBSTRATE RECOGNITION MECHANISM OF HUMAN β-ADRENARGIC RECEPTOR KINASE 1 BASED ON A THREE-DIMENSIONAL MODEL STRUCTURE. *Drug Des. Discovery* **1996**, *14*, 145−155.

(23) Knighton, D. R.; Zheng, J.; Ten Eyck, L. F.; Ashford, V. A.; Xuong, N. H.; Taylor, S. S.; Sowadski, J. M. Crystal Structure of the Catalytic Subunit of Cyclic Adenosine Monophosphate-Dependent Protein Kinase. *Science* **1991**, *253*, 407−414.

(24) Bouvier, M.; Collins, S.; O'Dowd, B. F.; Campbell, P. T.; de Blasi, A.; Kobilka, B. K.; MacGregor, C.; Irons, G. P.; Caron, M. G.; Lefkowitz, R. J. Two Distinct Pathways for cAMP-mediated Down-regulation of the β2-Adrenergic Receptor. Phosphorylation of the receptor and regulation of its mRNA level. *J. Biol. Chem.* **1989**, *264*, 16786−16792.

(25) Knighton, D. R.; Zheng, J.; Ten Eyck, L. F.; Xuong, N. H.; Taylor, S. S.; Sowadski, J. M. Structure of a Peptide Inhibitor Bound to the Catalytic Subunit of Cyclic Adenosine Monophosphate-Dependent Protein Kinase. *Science* **1991**, *253*, 414−420.

(26) Gray, N.; Detivaud, L.; Doerig, C.: Meijer, L. ATP-site directed inhibitors of cyclin-dependent kinases. *Curr. Med. Chem.* **1999**, *6*, 859−875.

(27) Mohammad, M.; McMahon, G.; Sun, L.; Tang, C.; Hirth, P.; Yeh, B. K.; Hubbard, SR.; Schlessinger, J. Structures of the Tyrosine Ktinase Dtomain of Fibroblast Growth Factor Receptor in Complex with Inhibitors. *Science* **1997**, *276*, 955−960.

(28) Iino, M.; Furugohri, T.; Fukuzawa, A.; Shibano, T. Asp278 of Human β-Adrenergic Receptor Kinase 1 Is Essential for Phosphorylation Activity. *Biochem. Biophys. Res. Commum.* **1997**, *239*, 548−551.

(29) *QUANTA*. Accelrys Inc.: 9685 Scranton Road, San Diego, CA 92121-3752, 2001.

(30) Janin, J.; Wodak, S.; Levitt, M.; Maigret, B. Conformation of Amino Acid Side-Chains in Proteins. *J. Mol. Biol.* **1978**, *125*, 357−386.

(31) Vasquez, M.; Nemethy, G.; Sheraga, H. A. Computed conformational states of the 20 naturally occurring amino acid residues and of the prototype residue α-aminobutyric acid. *Macromolecules* **1983**, *16*, 1043−1049.

(32) Baker, E. N.; Hubbard, R. E. Hydrogen bonding in globular proteins. *Prog. Biophys. Mol. Biol.* **1984**, *44*, 97−179.

(33) *CONVERTER*. Accelrys Inc.: 9685 Scranton Road, San Diego, CA 92121-3752, 2001.

(34) Crippen, G. M.; Havel, T. F. Stable Calculation of Coordinates from Distance Information. *Acta Crystallogr.* **1978**, *A34*, 282−284.

(35) Brooks, B. R.; Buccoleri, R. E.; Olafson, B. D.; States, D. J.; Swaminathan, S.; Karplus, M. CHARMM: A Program for Macromolecular Energy, Minimization, and Dynamics Calculations. *J. Comput. Chem.* **1983**, *4*, 187−217.

(36) Bohm, H. J. The development of a simple empirical scoring function to estimate the binding constant for a protein−ligand complex of known three-dimensional structure. *J. Comput.-Aided Mol. Des.* **1994**, *8*, 243−256.

(37) Jain, A. N. Scoring noncovalent protein−ligand interactions: A continuous differentiable function tuned to compute binding affinities. *J. Comput.-Aided Mol. Des.* **1996**, *10*, 427−440.

(38) Bohm, H. J. LUDI: rule-based automatic design of new substituents for enzyme inhibitor leads. *J. Comput.-Aided Mol. Des.* **1992**, *6*, 593−606.

(39) Head, R. D.; Smythe, M. L.; Oprea, T. I.; Waller, C. L.; Green, S. M.; Marshall, G. R. VALIDATE: A New Method for the Receptor-Based Prediction of Binding Affinities of Novel Ligands. *J. Am. Chem. Soc.* **1996**, *118*, 3959−3969.

(40) Wang, R.; Liu, L.; Lai, L.; Tang, Y. SCORE: A New Empirical Method for Estimating the Binding Afiinity of a Protein−Ligand Complex. *J. Mol. Model.* **1998**, *4*, 379−394.

(41) Koshland, D. E., Jr. Application of a theory of enzyme specificity to protein synthesis. *Proc. Natl. Acad. Sci. U.S.A.* **1958**, *44*, 98−104.

(42) Tsou, C. L. The role of active site flexibility in enzyme catalysis. *Biochemistry (Moscow)* **1998**, *63*, 253−258.

(43) Radmer, R. J.; Kollman, P. A. The application of three approximate free energy calculations methods to structure based ligand design: Trypsin and its complex with inhibitors. *J. Comput.-Aided Mol. Des.* **1994**, *8*, 243−256.

(44) Bossemeyer, D.; Engh, R. A.; Kinzel, V.; Ponstingl, H.; Huber, R. Phosphotransferase and substarte binding mechanism of the camp-dependent protein kinase catalytic subunit from porcine heart as deduced from the 2.0 Å structure of the complex with Mn2+ adenylyl imidodiphosphate and inhibitor peptide PKI(5-24). *EMBO J.* **1993**, *12*, 849−859.

(45) Narayana, N.; Cox, S.; Shaltiel, S.; Taylor, S. S.; Xuong, N. H. Crystal Structure of a Polyhistidine-Tagged Recombinant Catalytic Subunit of camp-Dependent Protein Kinase Complexed with the Peptide Inhibitor PKI(5-24) and Adenosine. *Biochemistry* **1997**, *36*, 4438−4448.

(46) Ring, C. S.; Cohen, F. E. Modeling protein structures: Construction and their applications. *FASEB J.* **1993**, *7*, 783−790.

(47) Lawrie, A. M.; Noble, M. E.; Tunnah, P.; Brown, N. R.; Johnson, L. N.; Endicott, J. A. Protein kinase inhibition by staurosporine revealed in details of the molecular interaction with CDK2. *Nat. Struct. Biol.* **1997**, *4*, 796−801.
(48) Lamers, M. B.; Antson, A. A.; Hubbard, R. E.; Scott, R. K.; Williams, D. H. Structure of the Protein Tyrosine Kinase Domain of C-terminal Src Kinase (CSK) in Complex with Staurosporine. *J. Mol. Biol.* **1999**, *285*, 713−725.
(49) *ISIS/Base*. MDL Information Systems, Inc.: 14600 Catalina Street, San Leandro, CA 94577, 2001.
(50) *InsightII, version 98.0*. Accelrys Inc.: 9685 Scranton Road, San Diego, CA 92121-3752, 2001.
(51) *Cerius2, version 4.5*. Accelrys Inc.: 9685 Scranton Road, San Diego, CA 92121-3752, 2001.
(52) Toledo, L. M.; Lydon, N. B.; Elbaum, D. The Structure-Based Design of ATP-Site Directed Protein Kinase Inhibitors. *Curr. Med. Chem.* **1999**, *6*, 775−805.
(53) *ACD*. MDL Information Systems, Inc. http://www.mdli.com/cgi/dynamic/product.html?uid=$uid&key=$key&id=17, 2000.
(54) Gasteiger, J.; Marsili, M. ITERATIVE PARTIAL EQUALIZATION OF ORBITAL ELECTRONEGATIVITY−A RAPID ACCESS TO ATOMIC CHARGES. *Tetrahedron* **1980**, *36*, 3219−3288.
(55) Sohlemann, P.; Hekman, M.; Buchen, C.; Elce, J. S.; Lohse, M. J. Purification and functional characterization of β-adrenergic receptor kinase expressed in insect cells. *FEBS Lett.* **1993**, *324*, 59−62.
(56) Pender, B. A.; Wu, X.; Axelsen, P. H.; Copperman, B. S. Toward a Rational Design of Peptide Inhibitors of Ribonucleotide Reductase: Structure−Function and Modeling Studies. *J. Med. Chem.* **2001**, *44*, 36−46.
(57) Honma, T.; Yoshizumi, T.; Hashimoto, N.; Hayashi, K.; Wakanishi, N.; Fukasawa, K.; Takaki, T.; Ikeura, C.; Ikuta, M.; Suzuki-Takahashi, I.; Hayama, T.; Nishimura, S.; Morishima, H. A Novel Approach for the Development of Selective Cdk4 Inhibitors: Library Design Based on Locations of Cdk4 Specific Amino Acid Residues. *J. Med. Chem.* **2001**, *44*, 4628−4640.
(58) Zheng, J. H.; Trafny, E. A.; Knighton, D. R.; Xuong, N. H.; Taylor, S. S.; Teneyck, L. F.; Sowadski, J. M. 2.2-Angstrom refinded crystal-structure of the catalytic subunit of cAMP-dependent protein-kinase complexed with Mn ATP and a peptide inhibitor. *Acta Crystallogr. D Biol. Crystallogr.* **1993**, *49*, 362−365.

JM010093A